

Switched Reluctance Motors with Concentrated Stator Windings and Salient Poles of Different Shape on Rotor

Nicoleta MEDREA, Ioan Adrian VIOREL, Member IEEE

SC EnergoBit SRL, Universitatea Tehnica Cluj-Napoca

Nicoleta.medrea@energobit.com, Ioan.adrian.viorel@mae.utcluj.ro

Abstract: Two structures of switched reluctance motors (SRMs) with concentrated stator windings and with salient poles on rotor of different shape are analyzed. An analytical model is proposed for both structures and a sizing-design algorithm developed. Two sample motors are designed and their performances calculated analytically and via two dimension finite element method (2D-FEM) are compared.

Index Terms: switched reluctance motor, salient poles, sizing-designing

I. INTRODUCTION

The switched reluctance motor (SRM) was one of the first electric motor to be patented, built and employed in a drive system by Davidson in 1838. The actual SRM with true electronically commuted phase supply synchronized with rotor position has been described by its essential features in the 70's last century. The various advantages of SRM make it an attractive alternative to DC and AC motors in some specific adjustable speed drives [1, 2, 3].

The conventional SRM has a basic structure that consists of salient poles on stator and on rotor with the magnetic circuit completed by a core back on both parts. The SRM's torque is produced by the tendency of its rotor to reach a position where the inductance and the flux produced by the energized stator winding are maximized.

The SRM's performances depend, like in the case of variable reluctance synchronous motor, on the difference between the phase flux linkage in aligned and unaligned rotor positions. Therefore, different solutions to enlarge this difference were proposed, one of them being a rotor with segments like for variable reluctance synchronous motor, [3, 4], another, presented here, with different rotor poles' shape.

Different variants of stator winding are suitable for a SRM with segmental or conventional rotor with salient poles. Some aspects concerning the SRM with segmental rotor performances function of the stator winding variant were analyzed [4, 5, 6]. Some of the conventional SRM analytical models, based on air-gap topology, are presented in [2, 3, 7, 8] and the sizing-design procedures have been developed too [3, 6, 7].

The analytical model of a SRM, independent of its rotor construction with salient poles or with segments, can be developed based on finite element method (FEM) analysis results [9, 10, 11].

In the paper an analytical model, based on the air-gap variable equivalent permeance concept, is presented in Section II. Such a model, which uses the air-gap geometrical data to define the equivalent permeance coefficient and the FEM results to calculate a saturation function that varies with the phase current and rotor position, has a large generality and can be applied to different rotor topologies.

Some practical considerations on the developed sizing-design procedure based on the analytical model presented are made in Section III and two sample SRMs are designed.

The sample SRMs performances are calculated via 2D-FEM analysis, the comparative results being presented and discussed in Section IV.

The final conclusions are given in Section V.

II. ANALYTICAL MATHEMATICAL MODEL

The SRMs analytical model developed here is based on the air-gap variable equivalent permeance concept [3, 10, 11], its coefficient, in a simplified form, being calculated function of the rotor structure in the air-gap. The saturation factor, introduced in the equivalent air-gap radial length, is calculated by using the results obtained via 2D-FEM analysis.

Since the stator magnetic field axis coincides with the stator phase axis, the air-gap variable equivalent permeance is [3, 10]:

$$P(\theta) = \frac{1}{g^*} (1 + P_R \sin \theta), \theta = Q_R \cdot \alpha \quad (1)$$

The equivalent air-gap, g^* , and the variable equivalent air-gap permeance P_R , are:

$$P_R = \frac{4}{\pi} \cdot \beta \cdot k_{CR} \cdot \sin \left(\frac{\gamma}{\beta} \cdot \frac{g}{\tau_R} \cdot \frac{\pi}{2} \right) \quad (2)$$

$$g^* = K_{CR} \cdot k_s \cdot g \quad (3)$$

$$\beta = \frac{(1-f)^2}{2(1+f^2)} \quad (4)$$

$$f = u + \sqrt{1+u^2} \quad (5)$$

$$u = b_{RS} / 2g$$

$$\gamma = \frac{4}{\pi} \left(u \cdot tg^{-1}u - \ln \sqrt{1+u^2} \right) \quad (6)$$

The Carter's factor K_{CR} considering slots only on rotor is:

$$K_{CR} = \frac{\tau_R}{\tau_R - \gamma \cdot g} \quad (7)$$

In the above equations, τ_R and b_{Rp} are the rotor pole pitch and pole width, g is the actual length of the motor air-gap, α is the actual rotor angular displacement and Q_R is the number of rotor poles.

A simplified form of the variable saturation function k_s , which depends on the phase current and rotor position, can be given by a cosinusoidal function as:

$$k_s(i, \theta) = k_{s0} \cdot (A \cdot \cos \theta + B) \quad (8)$$

The coefficients A and B are functions of phase current and should be calculated by using the aligned and unaligned flux linkage versus current characteristics obtained via 2D-FEM analysis.

For design purpose, in a first sizing-design stage, the saturation function can be reduced to a saturation constant, estimated in aligned position, considering the core material magnetization $B=f(H)$ characteristic. Accordingly, the saturation factor k_s is:

$$k_s = k_{s0} \cdot \frac{B_{uns}}{B_{sat}} \quad (9)$$

$$k_{s0} = 1 + \frac{1}{\mu_{r0}} \cdot \frac{l_{c0}}{l_g} \quad (10)$$

where B_{uns} , B_{sat} are the flux density unsaturated and saturated values, l_{c0} , l_g are the mean length of magnetic path in the iron-core and the air-gap respectively, and μ_{r0} is the initial relative permeability of the core material.

While B_{sat} is the corresponding value from $B=f(H)$ characteristic for the given H , the B_{uns} value is obtained from the equation which characterizes a straight line,

$$B = \mu_0 \cdot \mu_{r0} \cdot H \quad (11)$$

at the same given field intensity H value.

Since the air-gap flux density is:

$$B_g(\theta, i) = F \cdot \mu_0 \cdot P(\theta) \quad (12)$$

The air-gap flux-density maximum value, obtained in an aligned position, comes as:

$$B_{gmax}(i) = B_g(\theta, i)_{\theta=\pi/2} = F \cdot \mu_0 \cdot \frac{1}{g^*} (1 + P_R) \quad (13)$$

where F is the phase **mmf**.

The air-gap flux density is then:

$$B_g(\theta, i) = B_{gmax}(i) \frac{1 + P_R \sin \theta}{1 + P_R} \quad (14)$$

The inductance for one phase depends on the phase current and on the rotor position:

$$L(\theta, i) = M_d(i) \frac{1 + P_R \sin \theta}{1 + P_R} + L_{S\sigma} \quad (15)$$

The phase magnetizing inductance in aligned position, the d-axis value, is:

$$M_d(i) = \frac{B_{gmax}(i) \cdot N \cdot A_p}{i} \quad (16)$$

N is the phase turns number, i is the phase current, A_p is the stator pole area, and $L_{S\sigma}$ is the phase leakage inductance.

Calculating the flux linkage derivative, one obtains:

$$\begin{aligned} \frac{d\psi(\theta, i)}{dt} &= L(\theta, i) \frac{di}{dt} + i \frac{\partial L(\theta, i)}{\partial \theta} \cdot \frac{d\theta}{dt} \\ \omega &= \frac{d\theta}{dt} \end{aligned} \quad (17)$$

This leads to:

$$\begin{aligned} \frac{d\psi(\theta, i)}{dt} &= \left(M_d(i) \frac{1 + P_R \sin \theta}{1 + P_R} + L_{S\sigma} \right) \frac{di}{dt} + \\ &+ \omega M_d(i) \frac{P_R \cos \theta}{1 + P_R} \cdot i \end{aligned} \quad (18)$$

The electromagnetic torque developed by the motor, is:

$$T = \frac{\partial W'_m}{\partial \theta} = k_T \cdot i \cdot \cos \theta \quad (19)$$

Where:

$$k_T = \frac{N}{2} \cdot A_p \cdot \frac{P_R \cdot B_{gmax}}{1 + P_R} \cdot Q_R \quad (20)$$

The above presented analytical model is simple and useful in the sizing-design procedure developed for both types of the analyzed SRMs.

Through the analytic model presented above the induced **emf**, phase inductance on d- and q-axis and the electromagnetic torque are calculated based on the SRM's main dimensions, rated current and phase number of turns. The peak air-gap flux density value B_{gmax} is a design specification, as are the core material characteristics.

III. SIZING-DESIGNING PROCEDURE

Nowadays, the design procedure for any electric machine, SRM included, should consist of four compulsory stages:

- i) Sizing-designing stage to obtain general dimensions' initial values
- ii) FEM analysis of the electromagnetic structure
- iii) Heating-cooling calculation
- iv) Entire drive system simulation on computer

Previously to start the SRM's designing process one should answer to an important question concerning the phase number. The minimum phase number of a symmetrical SRM is three and there is no upper limit. By taking a larger number of phases the torque ripples can be reduced. Since the exterior diameter is limited in most cases, the designer must make an adequate compromise and adopt the minimum of three phases, but increase the number of stator poles to obtain a shorter flux path, and to assure the adequate slot area. For example, in this paper, a three phase conventional sample SRM was considered with 12 poles on stator and 8 on the rotor. A smaller number of rotor poles mean a reduced frequency at the same speed and consequently a reduced amount of iron-core losses.

A concentrated stator winding was adopted, each pole with its coil, four poles in quadrature for one phase. Such a structure assures short end windings and a lower leakage flux.

Against the conventional SRM rotor topology, or a segmental rotor discussed in [4, 5, 6] here a specific shape of the rotor poles is proposed in order to strongly reduce the flux linkage in unaligned position without a too important reduction of the aligned position phase flux linkage.

The SRM's sizing-designing procedure starts by calculating the average air-gap diameter, which is a function of [2, 3, 7]:

- i) Design specifications as rated output power, rated rotor speed and rated efficiency
- ii) Initially considered values for the stator electrical loading A_s and peak air-gap flux density B_{gmax} .
- iii) Adopted SRM's topology which means mainly the stator and rotor number of poles, rotor construction and stator phase winding
- iv) The value of the aspect ratio coefficient which represents the ratio between the stack length and the air-gap average diameter
- v) The initially taken values for some sizing constants and Carter's factor

The values of the stator electrical loading, of the peak air-gap phase density and of the sizing constants are taken considering the existing data, the motor topology and power and the iron core material. The aspect ratio coefficient value strongly depends on the drive requirements and should be taken as to assure, beside

the desired SRM geometry, the best ratio of the output torque to core losses.

Once the average air-gap diameter calculated and chosen the air-gap length, which depends on SRM's power, the main dimensions, as stack length, pole pitches and pole widths can be calculated. Considering the imposed rated current and chosen stator electrical loading a first value of the pole or phase, number of turns is calculated. This value should be checked via the induced **emf** calculation too.

Now the stator slot area results and the stator structure including the exterior motor's diameter, is completely defined. Initially the stator pole width can be equal to the stator slot opening and to the rotor pole width; these dimensions would be settled after the FEM analysis.

The phase induced **emf**, the phase inductances and the electromagnetic torque are calculated by using the equations obtained via proposed model, presented in the previous section.

TABLE I. Sample SRMs main dimensions.

	Rectangular poles	Trapezoidal poles
Mean air-gap diameter, mm	89.95	91.1
Stack axial length, mm	150	150
Air-gap flux density peak value, T	1.5	1.5
Air-gap length, mm	0.25	0.3
Slot fill factor	0.42	0.46
Stator tooth width, mm	12.05	11.93
Stator slot width, mm	11.5	11.92
Rotor tooth width, mm	12.09	5.92
Rotor slot width, mm	23.23	29.85
Rotor core back depth, mm	24.1	23.85
Stator core back depth, mm	10.6	11.9

The dimensions of the two sample SRMs obtained via the sizing-designing procedure, presented above and employing the actual analytical model, are given in Table 1.

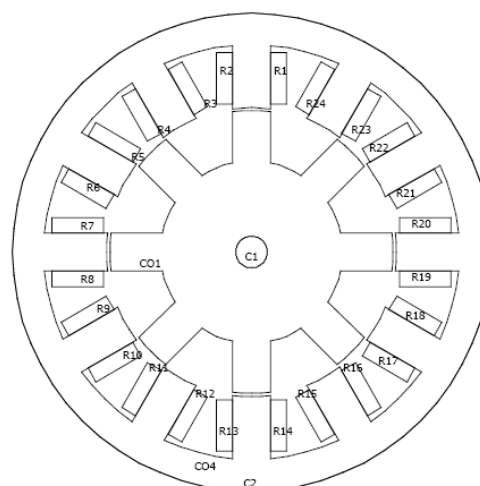


Fig. 1. SRM with rectangular rotor poles

The structures of the sample motors are presented in Figs 1 and 2.

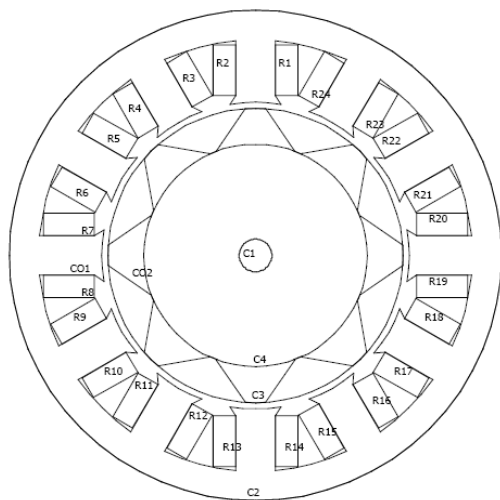


Fig. 2. SRM with trapezoidal rotor poles

In Fig. 1 the structure of the sample SRM with rectangular conventional rotor poles is given, the main domains for 2D-FEM calculation being:

- C1 – motor shaft
- CO1 – rotor structure
- CO4 – stator structure
- C2 – stator core
- R1 to R24 – windings

The sample SRM's structure, with trapezoidal rotor poles, is shown in Fig. 2. The main domains for 2D-FEM calculation are:

- C1 – motor shaft
- C2 – stator core
- C4 – rotor core
- C3 – rotor poles
- CO2 – rotor structure
- CO1 – stator structure

IV. CALCULATED RESULTS

The two SRM configurations, with the main dimensions given in Table 1, performances were calculated based on the usual sizing equations, [3, 7] for instance, and the developed analytical model. The main results obtained are presented in Table II.

TABLE II. Analytical results

	Rectangular poles	Trapezoidal poles
Resistance per phase (Ω)	1.728	1.823
Winding losses (W)	110.6	101.6
Core loss (W)	65.6	56.5
Electromagnetic torque (Nm)	32.22	33.117
Delivered power (kW)	2.024	2.081
Efficiency	0.914	0.923
Equivalent power factor	0.54	0.56

In order to compute magnetic field, 2D finite element method was used. The two configurations presented in Fig. 1 and in Fig. 2 were used for computing the magnetic flux lines. The results obtained from the simulation program employed are presented in the following.

The first configuration analyzed using FEM is the SRM with rectangular poles. Magnetic flux lines were considered for three positions of the rotor: aligned position, shown in Fig. 3, unaligned position, Fig. 4 and maximum torque position, Fig. 5.

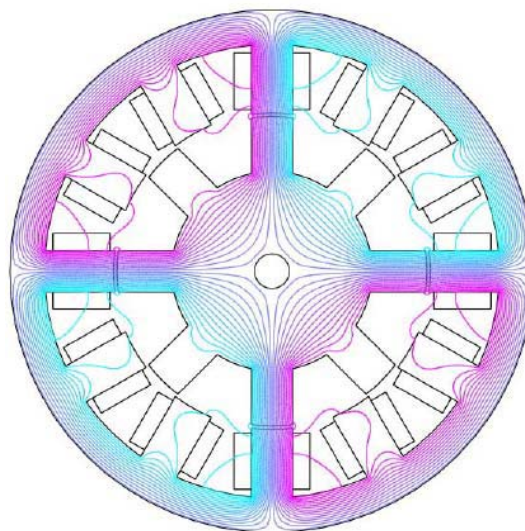


Fig. 3 SRM with rectangular poles – aligned position

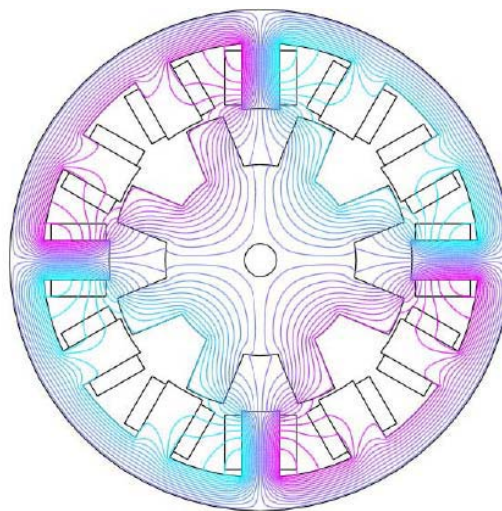


Fig. 4 SRM with rectangular poles – unaligned position

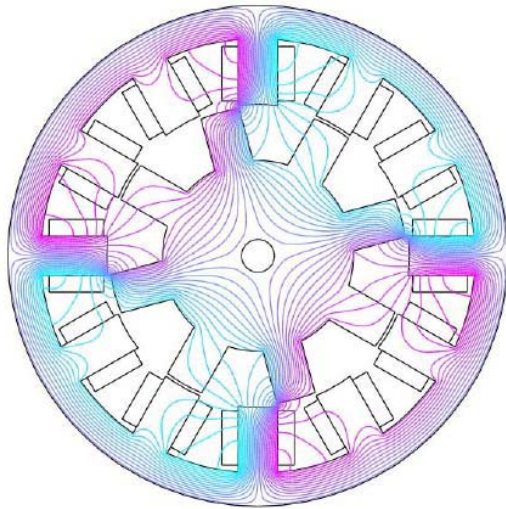


Fig. 5 SRM with rectangular poles – maximum torque position

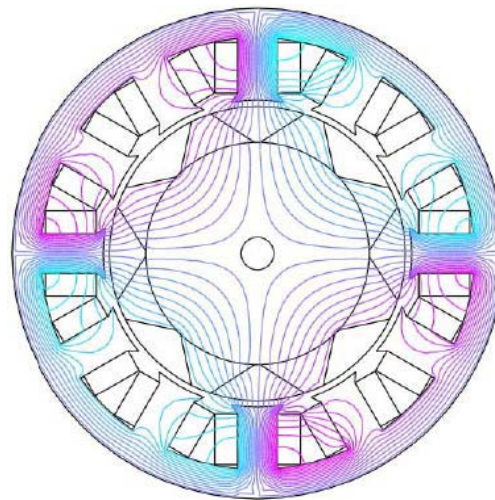


Fig. 7 SRM with trapezoidal poles – unaligned position

Next, the SRM configuration with trapezoidal rotor poles was studied via FEM analysis. Magnetic flux lines for the three positions, aligned position, Fig. 6, unaligned position, Fig. 7 and maximum torque position, Fig. 8, are presented too.

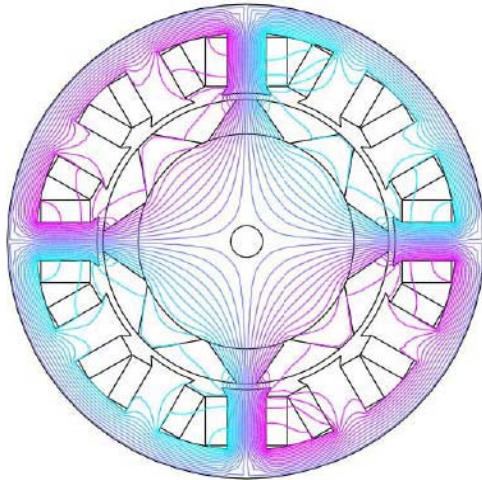


Fig. 6 SRM with trapezoidal poles – aligned position

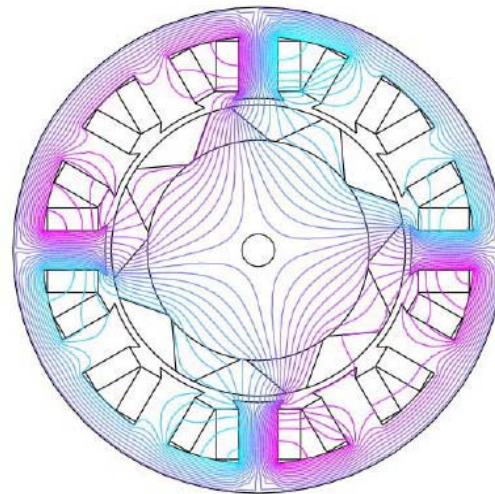


Fig. 8 SRM with trapezoidal poles – maximum torque position

Torque for different rotor positions was computed by using 2D FEM. The results are summarized in Table III, where α represents the rotor angular displacement.

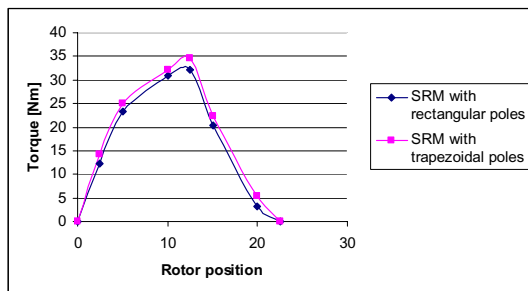


Fig. 9 Comparison for torque values

TABLE III. Torque as a function of rotor position

α	Torque (Rectangular poles) [Nm]	Torque (Trapezoidal poles) [Nm]
0	0	0
2.5	12.2669	14.1834
5	23.2658	25.1076
10	31.0055	32.1713
12.5	32.2573	34.4815
15	20.3493	22.2551
20	3.2185	5.4482
22.5	0	0

In Fig. 9 a comparison between the torque values obtained from FEM analysis for the sample SRMs is presented.

As one can see the differences between the peak torques values calculated via 2D-FEM and respectively analytic based on the developed model are small for the both sample SRMs considered. It proves the validity of the analytic model and shows that it is accurate enough.

In the sizing-design process the sample SRM with trapezoidal rotor poles has larger air-gap to avoid the rotor poles tip saturation. For the same reason the air-gap flux density peak value was taken only 1.5T, even if the iron core material would allow larger values.

V. CONCLUSIONS

A special trapezoidal topology of rotor poles for SRM is proposed in order to drastically reduce the unaligned flux linkage. A comparison between two similar sample SRMs with rectangular, respectively with trapezoidal rotor poles is made evincing the fact that the variant with trapezoidal rotor poles has better performances even if it has a 20% larger air-gap to avoid the saturation of the rotor poles tip. The two sample SRMs are designed based on a sizing – design procedure completed with an adequate analytic mathematic model which has a large generality. The calculations were done also by using 2D-FEM analysis, and the results stand by to sustain the accuracy of the analytic model.

As an overall conclusion it should be mentioned that this specific trapezoidal topology of the rotor poles offer the possibility to improve the SRM performances. In a further work the influence of the trapezoidal poles tip width will be presented and a suboptimal structure will be proposed.

Acknowledgments

The work was supported in part by SC EnergoBit SRL.

References

- [1] T.J.E. Miller, *Switched reluctance motors and their control*. Clarendon Press, Oxford, 1993
- [2] R. Krishnan, *Switched reluctance motors drives*. CRC Press, 2001
- [3] G. Hennenberger, I. A. Viorel, *Variable reluctance electrical machines*. Shaker Verlag, Aachen, Germany, 2001
- [4] B. C. Mecrow, J.W. Finch, E. A. El-Kharashi and A. G. Jack, "Switched reluctance motors with segmental rotors." IEE Proc. – Electr. Power Appl., vol. 149, no. 4, pp. 245-254, 2002
- [5] B. C. Mecrow, E. A. El-Kharashi, J.W. Finch and A. G. Jack, "Segmental rotor switched reluctance motors with single tooth windings." IEE Proc. – Electr. Power Appl., vol. 150, no. 5, pp. 591-599, 2003
- [6] B. C. Mecrow, J.W. Finch, E. A. El-Kharashi and A. G. Jack, "The design of switched reluctance motors with segmental rotors." In Proc. Int. Conf. on Electrical Machines, Brugge, Belgium, August 2002
- [7] V. A. Radun, "Design considerations for the switched reluctance motor." IEEE Trans on Industry Applications, vol. 31, no. 5, pp. 1079-1087, 1995
- [8] V.A. Radun, "Analytically computing the flux linked by switched reluctance motor phase when the stator and rotor poles overlap." IEEE Trans on Magnetics, vol. 36, pp. 1996-2003, 2000
- [9] H.-P. Chi, R.-L. Lin, J.-F. Chen, "Simplified flux-linkage model for switched reluctance motors". IEE Proc. Electr. Power Appl., vol. 152, no. 3, pp. 577-583, 2005
- [10] J. H. Chang, D. H. Kang, I. A. Viorel, L. Strete, „Transverse flux reluctance linear motor analytical model based on finite element method analysis results“. IEEE Trans on Magnetics, vol. 43, no. 4, pp. 1201-1204, 2007
- [11] C. J. Hwan, D. H. Kang, I. A. Viorel, I. Tomescu, L. Strete, "Saturated double salient reluctance motors analytical model". In Proc of Int. Conf. on Electrical Machines, Chanaia, Greece, September 2006.